crystals

MDPI

Article

Thermal Conductivity and Orientation Structure of Liquid Crystalline Epoxy Thermosets Prepared by Latent Curing Catalyst

Miyuki Harada * and Takuya Matsumoto

Department of Chemistry and Materials Engineering, Faculty of Chemistry, Materials and Bioengineering, Kansai University, Osaka 564-8680, Japan
* Correspondence: mharada@kansai-u.ac.jp

Abstract: Improvements in the performance of electronic devices necessitate the development of polymer materials with heat dissipation properties. Liquid crystalline (LC) epoxies have attracted attention because of the orientation of their polymer network chains and their resultant high thermal conductivity. In this study, a diglycidyl ether of 1-methyl-3-(4-phenylcyclohex-1-enyl)benzene was successfully synthesized as an LC epoxy and the LC temperature range was evaluated via differential scanning calorimeter (DSC). The synthesized LC epoxy was cured with *m*-phenylenediamine (*m*-PDA) as an amine-type curing agent and 1-(2-cyanoethyl)-2-undecylimidazole (CEUI) as a latent curing catalyst, respectively. The LC phase structure and domain size of the resultant epoxy thermosets were analyzed through X-ray diffraction (XRD) and polarized optical microscopy (POM). High thermal conductivity was observed in the *m*-PDA system (0.31 W/(m·K)) compared to the CEUI system (0.27 W/(m·K)). On the other hand, in composites loaded with 55 vol% Al_2O_3 particles as a thermal conductive filler, the CEUI composites showed a higher thermal conductivity value of 2.47 W/(m·K) than the *m*-PDA composites (1.70 W/(m·K)). This difference was attributed to the LC orientation of the epoxy matrix, induced by the hydroxyl groups on the alumina surface and the latent curing reaction.

Keywords: epoxy; thermosets; crosslinking; mechanical properties; thermal property; liquid crystals

Citation: Harada, M.; Matsumoto, T. Thermal Conductivity and Orientation Structure of Liquid Crystalline Epoxy Thermosets Prepared by Latent Curing Catalyst. *Crystals* **2024**, *14*, 47. https://doi.org/10.3390/cryst14010047

Academic Editors: Zhenghong He and Yuriy Garbovskiy

Received: 28 November 2023
Revised: 25 December 2023
Accepted: 26 December 2023
Published: 28 December 2023

1. Introduction

In recent years, as electronic devices have become more sophisticated and densely packaged, the amount of heat dissipated inside them has tended to increase. This causes functional failure and deterioration of peripheral components. Therefore, a need for higher thermal conductivity exists for encapsulating materials [1]. Epoxy resins are one of the conventional thermosetting polymers. They have been widely used in industrial fields, such as adhesives, coatings, and composite materials for their excellent bonding and thermal properties, chemical resistance, low shrinkage, processability, and electrical insulation properties. Therefore, epoxy resins are also used as encapsulation materials and printed circuit boards; however, general-purpose epoxy resins are known to have lower thermal conductivity than metallic and ceramic materials. In general, inorganic filler powders, such as alumina (Al_2O_3) [2–4] and boron nitride (BN) [5–12], are added to the resin matrix to attain encapsulating materials with high thermal conductivity. However, the extent to which composite fillers can improve thermal conductivity is limited because the increase in filler content causes matrix embrittlement and deterioration of molding processability because of high viscosity. Therefore, an urgent need exists to increase the thermal conductivity of the epoxy resin itself, which has been reported to further increase the thermal conductivity when it is filled with a filler.

Liquid crystalline (LC) epoxies with mesogen groups in the backbone moiety have received attention. Frequently, they contain azo, azomethine, ester, stilbene, biphenyl, and terphenyl as mesogenic groups. LC epoxies form LC structures such as nematic (N) and

smectic (S_m) phases via π–π stacking of mesogen groups. Not only in the monomeric state but also upon reaction with a curing agent, LC epoxies form LC domains in networked polymer chains. This oriented polymer structure efficiently suppresses phonon scattering and demonstrates superior thermal conductivity compared to general-purpose epoxy thermosets [13–34]. Akatsuka et al. have reported that an ester-type twin mesogen epoxy thermoset exhibits a thermal conductivity approximately four to five times higher than those of general-purpose epoxy resins [8]. Tokushige et al. reported that cured materials that form an S_m phase exhibit higher thermal conductivity than those that form an N phase [28]. However, in general, LC epoxy resin monomers with mesogen groups have a high melting point; thus, high-temperature conditions are critical during the preparation of cured products. However, high-temperature conditions have disadvantages, including high energy costs in industrial mass production. To solve this problem, we synthesized a phenylcyclohexene type LC epoxy with a low melting point and wide LC temperature range and subsequently found that the resultant thermosets exhibited high thermal conductivity [15].

Another possible curing method to improve LC alignment is the self-polymerization reaction of LC epoxy resins using a latent curing catalyst. Tertiary amine compounds and imidazole compounds are used as curing catalysts in the self-polymerization reaction of epoxy resins. These compounds are added to the epoxy resin in small amounts (1–5 phr). The cured LC epoxy thermosets prepared with a curing catalyst have a high concentration of mesogenic groups in their networked structure. However, there are imidazoles with a cyano group (–CN) [35] as a strong electron-withdrawing group. In addition, because of the lower electron density, imidazoles with a cyano group exhibit lower reactivity than conventional imidazole compounds. LC epoxy resins prepared with less-reactive curing agents have longer gelation times and can provide a range of possible mesogenic groups. We have also reported on the improvement of the alignment and toughness of cured materials using a mixture of LC epoxy resin and a rigid, highly reactive curing agent, where the curing agent was present in small amounts, contained flexible chains, and exhibited low reactivity [36]. The use of latent curing catalysts increased the concentration of mesogen groups in the LC epoxy thermosets and extended the gelation time, giving the mesogen groups more time to align; this alignment is expected to improve the orientation of networked polymer chains.

In the present study, a diglycidyl ether of 1-methyl-3-(4-phenylcyclohex-1-enyl)benzene as an LC epoxy monomer was synthesized and its LC property and reactivity were investigated. The differences in the LC phase structure and the thermal conductivity of the cured materials prepared using aromatic diamines as a curing agent and imidazoles as a latent curing catalyst were discussed. These properties were also compared with those of epoxy thermosets prepared with a conventional aromatic amine. The thermal conductivity of composites loaded with alumina particles as a high thermally conductive filler was also investigated.

2. Materials and Methods

2.1. Materials

The epoxy resin, curing agent, and curing catalyst used were diglycidyl ether of 1-methyl-3-(4-phenylcyclohex-1-enyl)benzene (DGEDPC-Me) (M_w = 392 g/mol, Cr 80 LC 132 Iso), *m*-phenylenediamine (*m*-PDA, M_w = 108 g/mol, m.p. 62–65 °C, Wako Pure Chemical Industries, Osaka, Japan), and 1-(2-cyanoethyl)-2-undecylimidazole (CEUI, M_w = 275 g/mol, m.p. 49–54 °C, Tokyo Kasei Chemical Industry, Tokyo, Japan), respectively. The structures of these chemicals are shown in Figure 1.

Al_2O_3 particles (AA-05, Sumitomo Chemical, particle mean diameter: 5 μm) were used as a thermal conductive filler.

Hexamethyl disilazane (HMDS, M_w = 275 g/mol, Tokyo Kasei Chemical Industry, Tokyo, Japan) was used as a silane decoupling agent for a glass substrate.

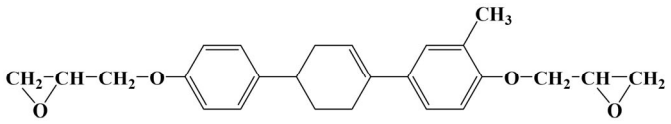

Diglycidyl ether of 1-methyl-3-(4-phenylcyclohex-1-enyl)benzene (DGEDPC-Me)

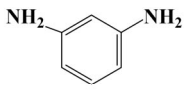

m-Phenylenediamine (*m*-PDA)

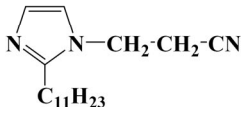

1-(2-Cyanoethyl)-2-undecylimidazole (CEUI)

Figure 1. Chemical structures of DGEDPC-Me, *m*-PDA, and CEUI.

2.2. Synthesis of 1,4-Diphenyl-3-Methyl-Cyclohexene-Type Epoxy Resin (DGEDPC-Me)

The DGEDPC-Me synthesis pathway is based on that reported in our previous study [32] on the same structure without the methyl branch. DGEDPC-Me was synthesized from a 24-times excess of 1-chloro-2,3-epoxypropane (119.64 g, 12.9 × 10^2 mmol, M_w = 93 g/mol; Wako Pure Chemical Industries, Osaka, Japan) and 4,4′-dihydroxy-(1-methyl-3-(4-phenylcyclohex-1-enyl)benzene) (15.00 g, 53.6 mmol, M_w = 280 g/mol; Honshu Chemical Industry, Tokyo, Japan) with 60 mL of dimethyl sulfoxide (DMSO) and tetra-*n*-butylammonium chloride (TBAC) (90.0 mg, 32.4 × 10^{-3} mmol, M_w = 278 g/mol, Sigma-Aldrich Co. LLC, St. Louis, MO, USA) as the catalyst. The epoxidation reaction was conducted at 60 °C for 1 h, after which a 50 wt% aqueous sodium hydroxide (M_w = 40 g/mol, Wako Pure Chemical Industries, Osaka, Japan) solution (5.15 g, 129 mmol) was added over 0.5 h and additionally reacted for 1.5 h to induce the epoxy ring-closure reaction. The product was purified through reprecipitation with 750 mL of methanol, followed by 5 washes with 20 mL of methanol. It was then dried at 60 °C for 2 h. The obtained product contained 15.69 g of white powder, and the reaction yield was 75%. All reagents in the above synthesis were used as received, without any purification. The structure of the synthesized compounds was confirmed using ^{1}H-NMR (JNM-AL 400; JEOL Ltd., Tokyo, Japan) and Fourier transform infrared (FT-IR, SPECTRUM 100, Perkin Elmer, Waltham, MA, USA) spectroscopy. The repeating unit was determined to be 0.06 via gel permeation chromatography (GPC, LC20AD, Shimadzu Corp., Kyoto, Japan) with THF as the eluent at 40 °C, using a refractive index detector (RID-20A, Shimadzu Corp., Kyoto, Japan). The sample (about 5 mg) was completely dissolved in 10 mL of THF.

^{1}H-NMR and FT-IR spectra are shown in Supplementary Materials Figures S1 and S2.

^{1}H-NMR ($CDCl_3$, δ, ppm): 1.9 (q, 2H, CH_2), 2.1 (d, 2H, CH_2), 2.3 (s, 3H, CH_3), 2.5 (t, 2H, CH_2), 2.8 (m, 1H, CH), 2.9 (d, 4H, CH_2, epoxy), 3.4 (m, 2H, CH, epoxy), 3.9 (d, 2H, CH_2, epoxy), 4.1 (d, 2H, CH_2, epoxy), 6.1 (s, 1H, CH), 6.7 (d, 2H, CH, aromatic), 6.9 (d, 2H, CH, aromatic), 7.1 (d, 2H, CH, aromatic), 7.2 (d, 2H, CH, aromatic), 7.3 (d, 2H, CH, aromatic).

IR (KBr, cm^{-1}): 3630–3095 (ν O–H), 3090–2900 (ν C–H, methylene), 2900–2790 (ν C–H, methyl), 1605, 1510 (ν C=C, aromatic), 1460 (δ C–H, methyl), 1390 (ν C–O, phenol), 1350 (δ C–H, methyl), 1030 (ν C–O, ether), 915 (ν C–O, epoxy).

The transition temperature of the synthesized DGEDPC-Me was measured with a differential scanning calorimeter (DSC Exter 7020, SII, Chiba, Japan) at a heating rate of 5 °C/min. The synthesized epoxy monomer was found to exhibit an LC phase between 80 and 132 °C (C 80 LC 132 I).

2.3. Curing of Epoxy Resin and Al_2O_3 Composites

DGEDPC-Me was cured with a stoichiometric amount (NH: epoxy group = 1:1) of the curing agent (*m*-PDA) or 3 phr of latent curing catalyst (CEUI). The epoxy resin was

completely melted at 160 °C for 2 min, and *m*-PDA or CEUI was then added. Both systems were cured in an oven at 70 °C for 3 h, at 80 °C for 1 h, and at 100 °C for 1 h. They were then cured at 220 °C for 0.5 h. The heating rate was 20 °C/min. The composites, loaded with Al_2O_3 particles (particle mean diameter: 5 μm) without any surface treatment, were prepared using the same procedure as above.

2.4. Surface Treatment of a Glass Substrate

The surface of a glass substrate was directly treated with HMDS at room temperature through the dry treatment method.

2.5. Characterization Techniques

The structure of the synthesized epoxy monomers and the conversion of the epoxy groups in their thermosets were analyzed through FT-IR spectroscopy (SPECTRUM 100, Perkin Elmer, MA, USA), using samples incorporated into KBr pellets. The resolution of the FT-IR spectrum was 4 cm^{-1}, and the spectra were collected after four scans. The chemical conversion of the epoxy groups was determined from the reduced size of the peak at 910 cm^{-1}, which was identified as an epoxy group. Here, the peak at 1510 cm^{-1}, which was identified as a benzene ring, was used as an internal standard.

The gel fraction was estimated on the basis of the change in weight of the powdered bulk samples (0.50 g). The samples in cylindrical filter paper were soaked and stacked in THF at 25 °C for 1 h, then at 40 °C for 1 h, and then at 60 °C for 1 h. Following extraction, the samples were fully dried at 60 °C for 6 h under vacuum, and their weight was subsequently measured.

The phase transition behavior and LC texture of the synthesized epoxy monomers and their thermosets were confirmed under cross-polarized light using a polarized optical microscope (POM; BH-2, Olympus Corporation, Tokyo, Japan) equipped with a hot stage (TPC-2000, Ulvac, Inc., Kanagawa, Japan); the samples were heated at 5 °C/min. The thickness of the thermoset samples was 10 μm.

The LC phase orientation in the epoxy thermosets was confirmed using wide-angle X-ray diffraction (WAXD; NANO-Viewer MicroMax-007HF, Rigaku Corporation, Tokyo, Japan) and an imaging plate detector (R-AXIS-IV, Rigaku Corporation, Tokyo, Japan). The layer spacing, d, was calculated using Bragg's formula ($n\lambda = 2d \cdot \sin\theta$). Diffraction patterns were obtained using Cu Kα (λ = 0.145 nm) radiation generated at 40 kV and 30 mA. The thickness of the epoxy thermoset samples was 1.0 mm.

The thermal conductivity at 25 °C was determined from the thermal diffusivity α, density ρ, and specific heat capacity C_p. The thermal conductivity λ was calculated using the following equation [37]:

$$\lambda = \alpha \cdot \rho \cdot C_p \quad (1)$$

The thermal diffusivity α of the systems at 25 °C was measured using Xe-flash analysis (LFA 447 NanoFlash, Netzsch, Selb, Germany) according to the ISO 18755 standard. The samples were prepared as disks with a diameter of 10.0 mm and thickness of 1.0 mm. The entire surface of the samples was coated with a Au layer of 500 Å via ion sputtering and then covered with a carbon layer of ~8 μm using a carbon sprayer (graphite coat; Nihon Senpaku) to enhance the thermal contact and prevent the direct transmission of light from the laser light source throughout the specimen. The measurement temperature was 25 °C.

The density ρ of the systems was measured at 25 °C using the pycnometer method according to the standard JIS K7112. The C_p was measured using a differential scanning calorimeter (DSC Exster 7020, SII, Chiba, Japan) at a heating rate of 5 °C/min. The sample weight was 10 mg, and the reference sample was α-Al_2O_3 (sapphire) (C_p: 0.78 J/(g·K)).

3. Results

3.1. Curing Reaction of the DGEDPC-Me/m-PDA and CEUI Systems

The conversion of the epoxy groups in the DGEDPC-Me systems was calculated through FT-IR measurements to confirm the effect of aromatic amine curing agents or latent

catalysts on reactivity (Figure 2). The results showed that the reactivity of the epoxy group in the aromatic amine *m*-PDA system was consumed rapidly, whereas the latent catalyst CEUI system showed a substantially lower reactivity in the initial stage of curing, and its reactivity gradually increased with increasing curing temperature. We speculate that the electron-withdrawing behavior of the cyano group of CEUI strongly suppressed the reactivity of the epoxy group.

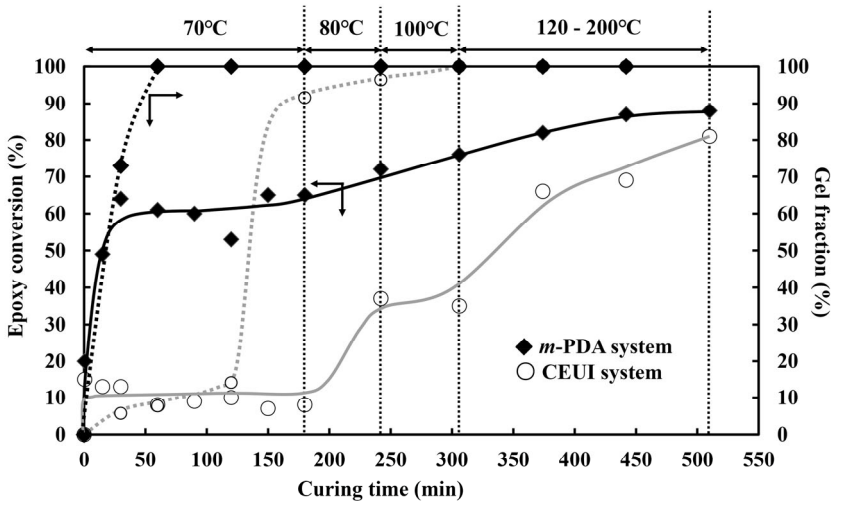

Figure 2. Epoxy conversion (solid line) and gel fraction (dotted line) of the (♦) *m*-PDA and (○) CEUI systems.

To confirm that the latent catalyst affects the extension of the gelation time, the gel fraction was measured during the curing process. As a result, in the CEUI system, extension of the gelation was observed with the latent catalyst, suggesting that the mesogenic groups had sufficient time for arrangement.

3.2. LC Phase Structure of the DGEDPC-Me/m-PDA and CEUI Systems

Figure 3 shows polarized optical micrographs collected during the curing process to investigate the differences in the liquid crystallinity of the DGEDPC-Me systems. The aromatic amine *m*-PDA system showed a dark field throughout the region at a curing time of 30 s immediately after melting, and an isotropic phase was formed temporarily. As the curing time progressed, a liquid-crystalline phase appeared after ~3 min and the growth of the LC domains was observed until ~10 min. However, the latent catalyst CEUI system showed an LC phase after melting, without isotropization. In addition, the LC phase was maintained even as the curing time progressed, and the LC domain diameter increased. The LC domains of the *m*-PDA system were ~60 μm, whereas those of the CEUI system were ~120 μm, indicating that larger domains were formed in the latent catalyst system. This result is attributable to the higher concentration of LC epoxy resin in the system. The concentration of mesogenic groups in the CEUI system with 3 phr catalyst added is higher than that in the *m*-PDA system because the aromatic amine was added on a chemical-equivalent basis. This chemical-equivalent addition of the aromatic amine is speculated to have improved the stacking effect between the mesogen groups and prolonged the gelation time by suppressing the reaction rate, thereby allowing the mesogen groups to self-align more easily.

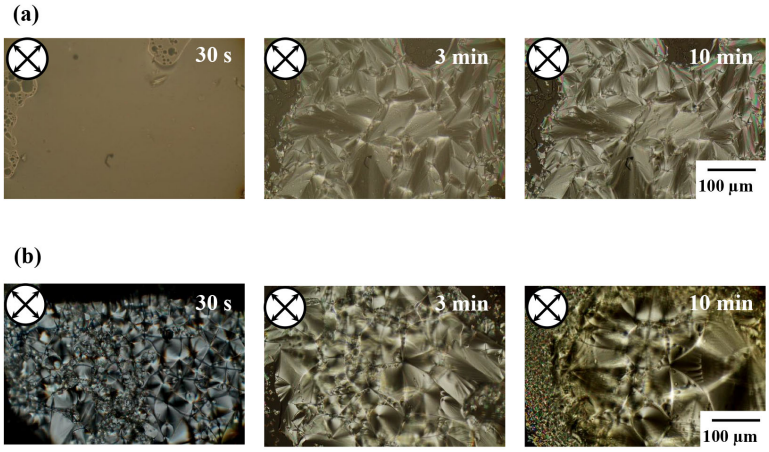

Figure 3. Polarized optical micrographs of the DGEDPC-Me thin films cured with (**a**) *m*-PDA and (**b**) CEUI systems during the curing process (curing temperature: 80 °C, magnification: ×200).

In addition, the bulk thermosets prepared in Al cups were polished to thin films and observed using POM (Figure 4). The birefringence pattern was confirmed in both systems under crossed Nicols, indicating that the LC phase was present in the DGEDPC-Me epoxy thermosets. When the crossed Nicols angle was rotated by 45°, the LC domains were identified as the area where bright and dark fields were switched. The results indicate that larger LC domains were formed in the CEUI (latent curing catalyst) system compared to those in the aromatic amine. A similar trend was confirmed in the bulk thermosets (Figure 3).

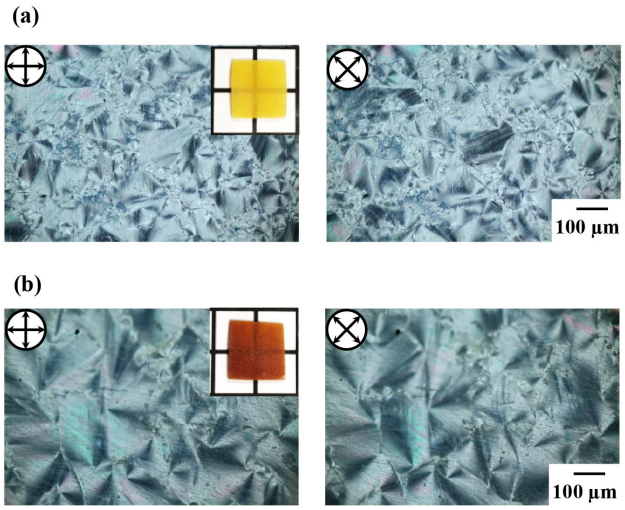

Figure 4. Polarized optical micrographs of the DGEDPC-Me cured with (**a**) *m*-PDA and (**b**) CEUI systems (magnification: ×100).

Figure 5 shows the XRD patterns acquired to identify the LC phase structure of the obtained LC epoxy thermosets cured through the m-PDA and CEUI. The results show a sharp peak at 2θ = 3.9° (2.26 nm) for (a) the *m*-PDA system and 4.4° (2.01 nm) for (b) the CEUI system on the small-angle side. Halos at 2θ = 18.4° (0.48 nm) were observed in the patterns of both systems. These results indicate that both systems formed an LC phase containing a S_m phase structure. The layer distance of the S_m phase formed by addition polymerization (*m*-PDA) and self-polymerization (CEUI) differed slightly. This result is attributable to the introduction of the amine curing agent by covalent bonding in the *m*-PDA system, resulting in a longer smectic layer distance than in the CEUI system. It reflects the difference in the assumed crosslinking structure. In addition, the relative intensity of the S_m (small-angle

side) peak to the halo intensity, based on the nematic phase or amorphous structure, was calculated as shown in Table 1. The higher this value, the greater the extent of alignment of the mesogenic groups. The higher relative intensity for the *m*-PDA system indicates that more of the S_m phase was formed, whereas the CEUI system formed more of the nematic phase. In our previous paper, we reported on the LC epoxy thermosets, the halo strength of which is significantly lower than that of its smectic peak [36]. Therefore, we think that the *m*-PDA and CEUI systems consist of a mixture of smectic and nematic phases.

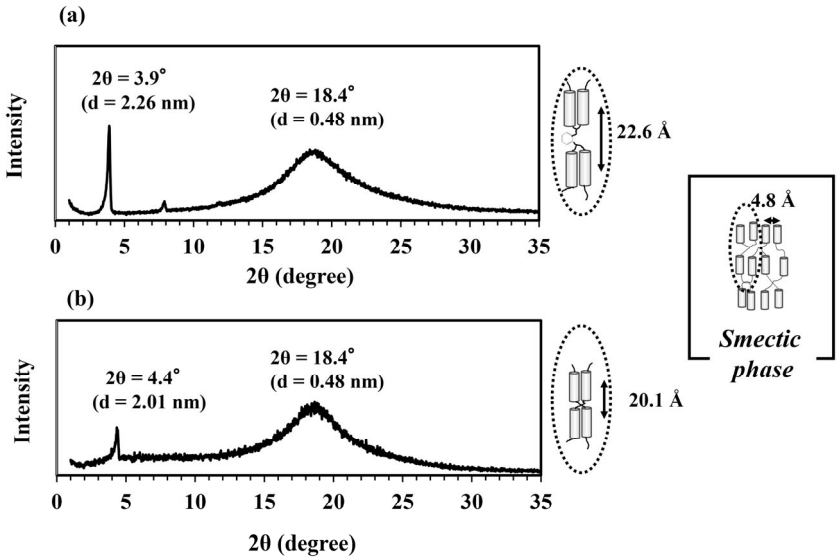

Figure 5. XRD patterns of the DGEDPC-Me cured with (**a**) *m*-PDA and (**b**) CEUI systems.

Table 1. Thermal conductivity of the DGEDPC-Me cured with the *m*-PDA and CEUI systems.

Curing System	Thermal Conductivity (W/(m·K))	Domain Size (μm)	Relative Intensity *
m-PDA system	0.31 ± 0.03	80	1.3
CEUI system	0.27 ± 0.02	120	0.7

* Calculated by $I_{3.9,\,4.4^\circ}/I_{Halo}$.

3.3. Thermal Conductivity of the DGEDPC-Me/m-PDA and CEUI Systems

The thermal conductivity of the LC epoxy thermosets cured through the m-PDA and CEUI is shown in Table 1. The results show that the *m*-PDA system exhibited a higher thermal conductivity (0.31 W/(m·K)) compared to the CEUI system (0.27 W/(m·K)). This higher thermal conductivity is attributed to the orientation structure of the networked polymer formed by the different curing reaction mechanisms. We have reported that the formation of the LC phase can be prevented with the loading of a BN filler [17]. However, Tanaka et al. reported that hydroxyl groups on the surface of glass substrates induced the formation of vertically oriented smectic phase structures when LC epoxy resin was cured with aromatic amine curing agents [25].

Here, the difference in the amount of hydroxyl groups in the formed networked polymer chains was investigated on the basis of the FT-IR measurements of both curing systems. More OH groups were formed in the *m*-PDA system than in the CEUI system. In the catalyst curing process, epoxy groups are consumed by the self-polymerization reaction derived from oxygen anions, resulting in an ether-linked network polymer. In this reaction, hydroxyl groups are hardly produced. However, the amine curing reaction generates one hydroxyl group per epoxy group because crosslinking occurs via addition polymerization of the amine and epoxy groups (Scheme 1). This difference in reaction mechanism results in a large difference in the amount of OH groups in these epoxy thermosets.

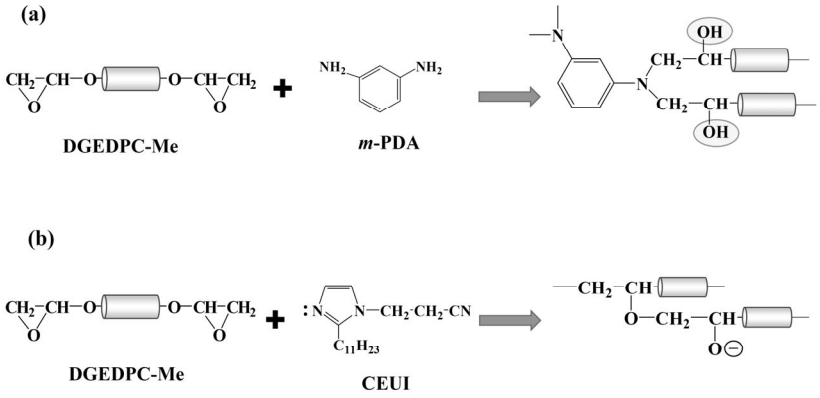

Scheme 1. Curing reaction of the DGEDPC-Me cured with (**a**) *m*-PDA and (**b**) CEUI systems.

3.4. Alignment of the DGEDPC-Me/m-PDA and CEUI Systems on Glass Substrates

We conducted a model experiment to investigate the influence of the amount of hydroxyl groups formed by the reaction on the orientation of mesogen groups in the thermosets. The *m*-PDA system, which forms hydroxyl groups via a crosslinking reaction, and the CEUI system, which generates almost no hydroxyl groups, were cured on a glass substrate with hydroxyl groups on its surface. We investigated whether the OH groups present on the outside induced the alignment of mesogen groups in the reticular chains of the CEUI system. Figure 6 shows the results of X-ray diffraction measurements of LC epoxy cured on a glass substrate. As a result, a sharp, high-intensity peak at $2\theta \approx 4^\circ$ and a low-intensity halo at $2\theta \approx 18^\circ$ were observed in the patterns of both the *m*-PDA and CEUI systems, indicating that, compared to the bulk thermosets, the CEUI system formed a larger amount of smectic phase structures. This result suggests that the presence of external hydroxyl groups leads to the alignment of mesogen groups in the CEUI system, which generates almost no hydroxyl groups.

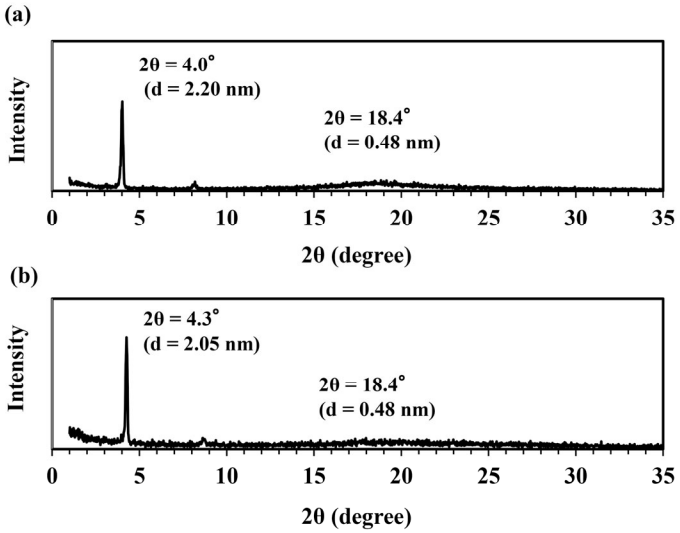

Figure 6. XRD patterns of the DGEDPC-Me cured with (**a**) *m*-PDA and (**b**) CEUI systems on glass substrates.

For further comparative study, we subjected glass substrates to a hydrophobic surface treatment using hexamethylene disilazane (HMDS). The DGEDPC-Me/CEUI system was cured on the hydrophobic glass substrates. The results of XRD measurements of the system are shown in Figure 7. Small-angle peaks derived from the smectic phase structure were identified. The system of the board showed lower values. This finding is attributable to the hydrophobic surface treatment substantially reducing the hydroxyl groups, making an

arrangement of mesogenic groups difficult. These results confirmed that more hydroxyl groups on the substrate surface led to better mesogen group orientation. Tanaka et al. have reported that the LC epoxy orientation is induced by the formation of hydrogen bonds between the hydroxyl groups formed by the ring-opening reaction of epoxy groups and the hydroxyl groups on the surface of the glass substrate [25]. However, the results in Figures 6 and 7 indicate that the LC orientation is induced by interaction with the substrate even in the catalyst curing system, which generates a small amount of hydroxyl groups in the curing reaction.

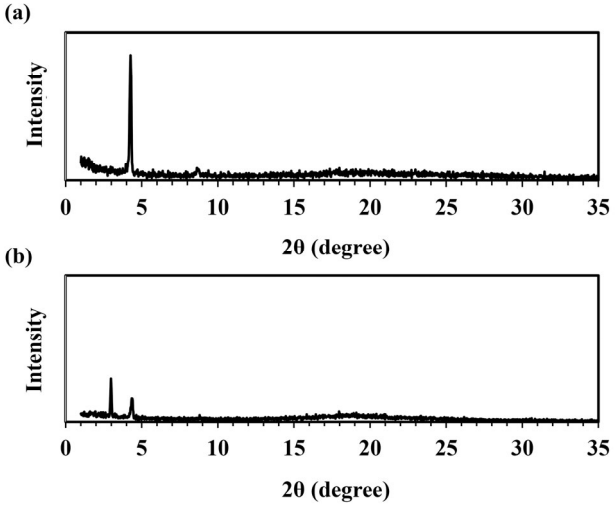

Figure 7. XRD patterns of CEUI systems cured on glass substrates. (**a**) Untreated and (**b**) treated with HMDS.

3.5. Thermal Conductivity of the DGEDPC-Me/m-PDA and CEUI/Al_2O_3 Composites

The DGEDPC-Me composites loaded with alumina particles having hydroxyl groups on the surface were prepared for the *m*-PDA and CEUI systems. On the basis of the results of the model experiment on the hydrophilic glass surface in Figure 7, we expected the S_m phase orientation-induced effect of the mesogen groups in the networked chains to influence the surface of the alumina filler, especially in the CEUI system. Figure 8 shows the relationship between the thermal conductivity of the resultant composites and the volume fraction of Al_2O_3 particle. The results show that the thermal conductivity of both the *m*-PDA and CEUI systems improved dramatically with increasing addition of alumina particles. It is noteworthy that the CEUI composites loaded with 55 vol% Al_2O_3 particles showed a higher thermal conductivity value of 2.47 W/(m·K) than the *m*-PDA composites (1.70 W/(m·K)). A substantial improvement in thermal conductivity was observed in the CEUI system in particular, despite the lower thermal conductivity of the unloaded system. This result is attributable to the hydroxyl groups on the surface of the dispersed alumina particles improving the orientation of the mesogen groups in the CEUI system. In addition, the latent curing catalyst might have suppressed the initial curing reactivity, resulting in delayed gelation, providing sufficient time for orientation induction.

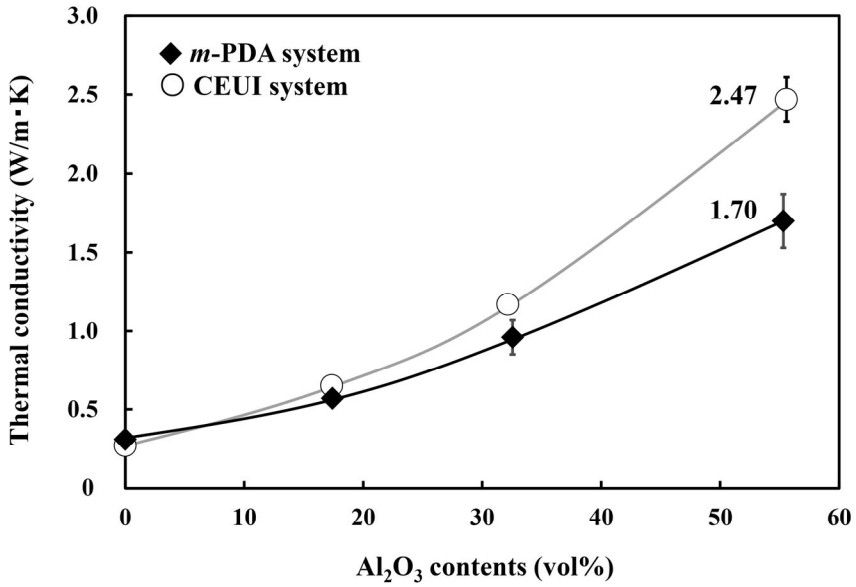

Figure 8. Thermal conductivity of the DGEDPC-Me cured with (♦) *m*-PDA and (○) CEUI systems loaded with Al_2O_3 (5 μm).

4. Conclusions

A diglycidyl ether of 1-methyl-3-(4-phenylcyclohex-1-enyl)benzene was cured using both *m*-PDA as an aromatic amine and CEUI as a latent curing catalyst. The CEUI catalyst system showed a long gelation time in the curing process and the obtained epoxy thermoset formed larger LC domains than the *m*-PDA system. However, the smectic LC orientation in the CEUI system was poorer than that in the *m*-PDA system. The thermal conductivity of the CEUI system was 0.27 W/(m·K), and the value was low compared to that of the *m*-PDA system (0.31 W/(m·K)). In addition, composites loaded with alumina particles were prepared for both the *m*-PDA and CEUI systems. Though the thermal conductivity of both systems improved with increasing addition of alumina particles, a substantial improvement in thermal conductivity was observed in the CEUI system. Even in the CEUI system, which had almost no hydroxyl groups, the delayed gelation and the hydroxyl groups on the alumina surface improved the mesogen group alignment and the thermal conductivity of the composite.

Supplementary Materials: The following supporting information can be downloaded at: https://www.mdpi.com/article/10.3390/cryst14010047/s1. Figure S1. ^{1}H-NMR spectra of the DGEDPC-Me (a) before and (b) after epoxidation; Figure S2. FT-IR spectra of the DGEDPC-Me (a) before and (b) after epoxidation.

Author Contributions: Conceptualization, methodology, formal analysis, investigation, writing original draft preparation, M.H.; data curation, M.H. and T.M.; writing—review and editing, M.H.; project administration, M.H. All authors have read and agreed to the published version of the manuscript.

Funding: This research received no external funding.

Data Availability Statement: The data presented in this study are available in this article and supplementary material.

Conflicts of Interest: The authors declare no conflicts of interest.

References

1. Lee, H.; Smet, V.; Tummala, R. Review of packaging schemes for power module. *IEEE J. Emerg. Sel. Top. Power Electron.* **2020**, *8*, 1.
2. Yetgin, H.; Veziroglu, S.; Aktas, O.; Yalçinkaya, T. Enhancing thermal conductivity of epoxy with a binary filler system of h-BN platelets and Al_2O_3 nanoparticles. *Int. J. Adhes. Adhes.* **2020**, *98*, 102540. [CrossRef]
3. Li, H.; Zheng, W. Enhanced thermal conductivity of epoxy/alumina composite through multiscale-disperse packing. *J. Compos. Mater.* **2021**, *55*, 17–25. [CrossRef]

4. Tian, F.; Cao, J.; Ma, W. Enhanced thermal conductivity and rheological performance of epoxy and liquid crystal epoxy composites with filled Al_2O_3 compound. *Polym. Test.* **2023**, *120*, 107940. [CrossRef]
5. Liu, Z.; Li, J.; Liu, X. Novel functionalized BN nanosheets/epoxy composites with advanced thermal conductivity and mechanical properties. *ACS Appl. Mater. Interfaces* **2020**, *12*, 6503–6515. [CrossRef] [PubMed]
6. Wang, Z.; Zhang, T.; Wang, J.; Yang, G.; Li, M.; Wu, W. The investigation of the effect of filler sizes in 3D-BN skeletons on thermal conductivity of epoxy-based composites. *Nanomaterials* **2022**, *12*, 446. [CrossRef] [PubMed]
7. Du, X.; Yang, W.; Zhu, J.; Fu, L.; Li, D.; Zhou, L. Aligning diamond particles inside BN honeycomb for significantly improving thermal conductivity of epoxy composite. *Compos. Sci. Technol.* **2022**, *222*, 109370. [CrossRef]
8. Yu, C.; Zhang, J.; Li, Z.; Tian, W.; Wang, L.; Luo, J.; Li, Q.; Fan, X.; Yao, Y. Enhanced through-plane thermal conductivity of boron nitride/epoxy composites. *Compos. Part A* **2017**, *98*, 25–31. [CrossRef]
9. Bian, W.; Yao, T.; Chen, M.; Zhang, C.; Shao, T.; Yang, Y. The synergistic effects of the micro-BN and nano-Al_2O_3 in micro-nano composites on enhancing the thermal conductivity for insulating epoxy resin. *Compos. Sci. Technol.* **2018**, *168*, 420–428. [CrossRef]
10. Yang, X.; Zhu, J.; Yang, D.; Zhang, J.; Guo, Y.; Zhong, X.; Kong, J.; Gua, J. High-efficiency improvement of thermal conductivities for epoxy composites from synthesized liquid crystal epoxy followed by doping BN fillers. *Compos. Part B Eng.* **2020**, *185*, 107784. [CrossRef]
11. Wu, L.; Huang, Y.; Yeh, Y.; Li, C. Characteristic and Synthesis of High-Temperature Resistant Liquid Crystal Epoxy Resin Containing Boron Nitride Composite. *Polymers* **2022**, *14*, 1252. [CrossRef] [PubMed]
12. Bao, Q.; He, R.; Liu, Y.; Wang, Q. Multifunctional boron nitride nanosheets cured epoxy resins with highly thermal conductivity and enhanced flame retardancy for thermal management applications. *Compos. Part A* **2023**, *164*, 107309. [CrossRef]
13. Akatsuka, M.; Takezawa, Y. Study of high thermal conductive epoxy resins containing controlled high-order structures. *J. Appl. Polym. Sci.* **2003**, *89*, 2464–2467. [CrossRef]
14. Harada, M.; Ochi, M.; Tobita, M.; Kimura, T.; Ishigaki, T.; Shimoyama, N.; Aoki, H. Thermal-conductivity properties of liquid-crystalline epoxy resin cured under a magnetic field. *J. Polym. Sci. Part A Polym. Phys.* **2003**, *41*, 1739–1743. [CrossRef]
15. Tokushige, N.; Mihara, T.; Koide, N. Thermal properties and photo-polymerization of diepoxy monomers with mesogenic group. *Mol. Cryst. Liq. Cryst.* **2005**, *428*, 33–47. [CrossRef]
16. Song, S.; Katagi, H.; Takezawa, T. Study on high thermal conductivity of mesogenic epoxy resin with spherulite structure. *Polymer* **2012**, *53*, 4489–4492. [CrossRef]
17. Harada, M.; Hamaura, N.; Ochi, M.; Agari, Y. Thermal conductivity of liquid crystalline epoxy/BN filler composites having ordered network structure. *Compos. Part B* **2013**, *55*, 306–313. [CrossRef]
18. Li, Y.; Badrinarayanan, P.; Kessler, M. Liquid crystalline epoxy resin based on biphenyl mesogen: Thermal characterization. *Polymer* **2013**, *54*, 3017–3025. [CrossRef]
19. Giang, T.; Kim, J. Effect of backbone moiety in diglycidylether-terminated liquid crystalline epoxy on thermal conductivity of epoxy/alumina composite. *J. Ind. Eng. Chem.* **2015**, *30*, 77–84. [CrossRef]
20. Guo, H.; Zheng, H.; Gan, J.; Liang, L.; Wu, K.; Lu, M. High thermal conductivity epoxies containing substituted biphenyl mesogenic. *J. Mater. Sci. Mater. Electron.* **2016**, *27*, 2754–2759. [CrossRef]
21. Kawamoto, S.; Fujiwara, H.; Nishimura, S. Hydrogen characteristics and ordered structure of mono-mesogen type liquid-crystalline epoxy polymer. *Int. J. Hydrog. Energy* **2016**, *41*, 7500–7510. [CrossRef]
22. Guo, H.; Lu, M.; Liang, L.; Wu, K.; Ma, D.; Xue, W. Liquid crystalline epoxies with lateral substituents showing a low dielectric constant and high thermal conductivity. *J. Electron. Mater.* **2017**, *46*, 982–991. [CrossRef]
23. Kim, Y.; Yeo, H.; You, N.; Jang, S.G.; Ahn, S.; Jeong, J.; Lee, S.H.; Goh, M. Highly thermal conductive resins formed from wide-temperature-range eutectic mixtures of liquid crystalline epoxies bearing diglycidyl moieties at the side positions. *Polym. Chem.* **2017**, *8*, 2806–2814. [CrossRef]
24. Tanaka, S.; Hojo, F.; Takezawa, Y.; Kanie, K.; Muramatsu, A. Layer structure formation of mesogenic liquid crystalline epoxy resin during curing reactions: A reactive coarse-grained molecular dynamics study. *Polym.-Plast. Technol. Eng.* **2018**, *57*, 269–275. [CrossRef]
25. Tanaka, S.; Hojo, F.; Takezawa, Y.; Kanie, K.; Muramatsu, A. Homeotropically aligned monodomain-like smectic-A structure in liquid crystalline epoxy films: Analysis of the local ordering structure by microbeam small-angle X-ray scattering. *ACS Omega* **2018**, *3*, 3562–3570. [CrossRef] [PubMed]
26. Jeong, I.; Kim, C.B.; Kang, D.; Jeong, K.; Jang, S.G.; You, N.; Ahn, S.; Lee, D.; Goh, M. Liquid crystalline epoxy resin with improved thermal conductivity by intermolecular dipole–dipole interactions. *J. Polym. Sci. Part A Polym. Chem.* **2019**, *57*, 708–715. [CrossRef]
27. Ota, S.; Yamaguchi, K.; Harada, M. Phase structure and thermal conductivity of liquid crystalline epoxy resins cured with the binary mixed curing agents. *J. Netw. Polym. Jpn.* **2019**, *40*, 278–286.
28. Lin, Z.; Cong, Y.; Zhang, B.; Huang, H. Synthesis and characterization of a novel Y-shaped liquid crystalline epoxy and its effect on isotropic epoxy resin. *Liq. Cryst.* **2019**, *46*, 1467–1477. [CrossRef]
29. Shen, W.; Cao, Y.; Zhang, C.; Yuan, X. Network morphology and electro-optical characterization of epoxy based polymer stabilized liquid crystals. *Liq. Cryst.* **2020**, *47*, 481–488. [CrossRef]
30. Ota, S.; Harada, H. Filler surface adsorption of mesogenic epoxy for LC Epoxy/MgO composites with high thermal conductivity. *Compos. Part C Open Access* **2021**, *4*, 100087. [CrossRef]

31. Ota, S.; Harada, M. Thermal conductivity enhancement of liquid crystalline epoxy/MgO composites by formation of highly ordered network structure. *J. Appl. Polym. Sci.* **2021**, *138*, 50367. [CrossRef]
32. Harada, M.; Kawasaki, Y. High toughness and thermal conductivity of thermosets from liquid crystalline epoxy with low melting point. *J. Appl. Polym. Sci.* **2022**, *139*, 52391. [CrossRef]
33. Zhong, X.; Yang, X.; Ruan, K.; Zhang, J.; Zhang, H.; Gu, J. Discotic Liquid Crystal Epoxy Resins Integrating Intrinsic High Thermal Conductivity and Intrinsic Flame Retardancy. *Macromol. Rapid Commun.* **2022**, *43*, 2100580. [CrossRef]
34. Hossain, M.; Olamilekan, A.; Jeong, H. Diacetylene-containing dual-functional liquid crystal epoxy resin: Strategic phase control for topochemical polymerization of diacetylenes and thermal conductivity enhancement. *Macromolecules* **2022**, *55*, 11, 4402–4410. [CrossRef]
35. Wang, M.; Yu, Y.; Wu, X.; Li, S. Synthesis and properties of cycloaliphatic epoxy resins containing imide and diphenyl sulfone. *Polymer* **2004**, *45*, 1253–1259. [CrossRef]
36. Harada, M.; Yamaguchi, K. Fracture toughness of highly ordered liquid crystalline epoxy thermosets achieved by optimized composition of curing agents. *J. Appl. Polym. Sci.* **2021**, *138*, 50593. [CrossRef]
37. Van Krevelen, D.; Te Nijenhuis, K. *Properties of Polymers*, 4th ed.; Elsevier: Oxford, UK, 2009.